

Two-dimensional rogue waves on zero background of the Davey-Stewartson II equation

Lijuan Guo¹, Jingsong He^{2*}, Lihong Wang³, Yi Cheng¹, D.J. Frantzeskakis⁴, P.G. Kevrekidis⁵

¹ School of Mathematical Sciences, University of Science and Technology of China, Hefei, Anhui 230026, P. R. China

² Institute for Advanced Study, Shenzhen University, Shenzhen, Guangdong 518060, P. R. China

³ School of Mathematics and Statistics, Ningbo University, Ningbo, Zhejiang 315211, P. R. China

⁴ Department of Physics, University of Athens, Panepistimiopolis, Zografos, Athens 15784, Greece

⁵ Department of Mathematics and Statistics, University of Massachusetts, Amherst, MA 01003-4515, USA *

A prototypical example of a rogue wave structure in a two-dimensional model is presented in the context of the Davey-Stewartson II (DS II) equation arising in water waves. The analytical methodology involves a Taylor expansion of an eigenfunction of the model's Lax pair which is used to form a hierarchy of infinitely many new eigenfunctions. These are used for the construction of two-dimensional (2D) rogue waves (RWs) of the DS II equation by the even-fold Darboux transformation (DT). The obtained 2D RWs, which are localized in both space and time, can be viewed as a 2D analogue of the Peregrine soliton and are thus natural candidates to describe oceanic RW phenomena, as well as ones in 2D fluid systems and water tanks.

Introduction. A two-dimensional (2D) rogue wave (RW) is a short-lived large amplitude wave, which is doubly localized in two spatial variables, x and y (as well as in time), and its modulus is a rational function. Naturally, a RW of a suitable 2D partial differential equation can provide a genuine dynamical paradigm of the oceanic RWs [1–3], and also be of relevance to other areas of physics, including nonlinear optics and atomic Bose-Einstein condensates [4]. However, any analytical form of such a genuine 2D RW has not been reported so far.

A candidate model that may give rise to purely 2D RWs, which in turn may describe oceanic extreme events, is the Davey-Stewartson II (DS II) system [5]:

$$\begin{aligned} iu_t + u_{xx} - u_{yy} + (2\kappa|u|^2 + S)u &= 0, \\ S_{xx} + S_{yy} &= -4\kappa(|u|^2)_{xx}, \quad \kappa = \pm 1. \end{aligned} \quad (1)$$

In the context of water waves, $u(x, y, t)$ is the amplitude of a surface wave packet, and $S(x, y, t)$ is the velocity potential of the mean flow interacting with the surface wave; in fact, u is proportional to the amplitude of the first harmonic and S the mean (zeroth harmonic) in the slowly-varying envelope expansion. The fluid velocity potential ϕ can then be reconstructed as $\phi \sim S(x, y, t) + F[u(x, y, t)\exp(ikx - i\omega t) + \text{c.c.}]$, where c.c. stands for the complex conjugate and $F = \cosh(k(z+h))/\cosh(kh)$; k is the wavenumber, ω the frequency and h represents the depth. Finally, parameter κ sets, in general, the type of nonlinearity: $\kappa = \pm 1$ corresponds to defocusing and focusing cases; in the water wave problem, $\kappa = -1$. This model describes two-dimensional water waves with a weak surface tension [5–7] (see also the reviews [8, 9] and Ref. [10] for a rigorous justification).

The DS II equation is the integrable 2D extension of the famous nonlinear Schrödinger (NLS) equation [11, 12]. The latter, is known to possess one-dimensional

(1D) rational RWs, i.e., the fundamental RW in the form of the so-called Peregrine soliton [13–15], as well as other higher-order RWs [16–19], which have been observed in optical systems and water tank experiments [20–26]. Since the DS II equation can be viewed as a non-local hyperbolic NLS equation, it should be mentioned that its local counterpart, i.e., the 2D hyperbolic NLS, has been computationally explored in [27] in the context of deep water gravity waves, with the numerical results suggesting that RWs may persist in such settings.

The main focus of the present work is to offer *explicit analytical solutions* for the DS II RWs, which can be viewed as the prototypical generalization of Peregrine RWs to genuinely higher dimensional settings. The ubiquitous relevance of such settings in physical applications highlights the importance of a systematic toolbox enabling the identification of such solutions. While the importance of this problem has been recognized and other mathematically motivated (from integrability theory) 2D extensions of RWs have been proposed [28], the present 2D RW proposal constitutes a prototypical physically relevant example in view of the above remarks.

Before proceeding, we review some key properties of the DS II equation. First we note that it is a completely integrable system via the inverse scattering transform (IST), and particularly by means of the so-called $\bar{\partial}$ -method [29–31]. In addition, the DS II equation, apart from the context of water waves, plays an important role in a variety of other physical settings, including plasma physics [32–34], nonlinear optics [35–37], and ferromagnets [38]. Regarding its solutions, the defocusing DS II equation ($\kappa = +1$), does not possess lump solutions [39], while the focusing DS II equation ($\kappa = -1$) not only possesses lump solutions [29, 40, 41], but also line rogue waves [42] (localized only in one spatial variable), and lump-line soliton solutions [43]. The N -lump solution in Ref. [41] displays simple interaction dynamics, namely lumps recover their original velocity and shape without a phase shift after their interaction. On the other hand, the multi-pole lumps of the DS II equation [44, 45] feature nontrivial interaction dynamics, and

* Email of corresponding author: hejingsong@szu.edu.cn, jshe@ustc.edu.cn

decay as r^{-N} ($N \geq 2$), $r^2 = x^2 + y^2$. This kind of lumps [45] corresponds to a discrete spectrum whose related eigenfunctions have higher-order poles in the spectral variable in the framework of IST. The multi-pole lumps were also found in other 2D integrable equations, such as the Kadomtsev-Petviashvili I (KP I) equation [46] and Fokas equation [47]. Note that the periodic soliton resonance of the DS II equation has also been studied in Refs. [48, 49]. This broad spectrum of recent activity showcases the wide interest in this class of models.

Although there exist many results on the solutions of the DS II equation, the construction of 2D RWs for this equation, is still an open problem, strongly motivated by (a) modeling analytically 2D RWs in the ocean (or in a large water tank), and (b) finding a 2D analogue of the Peregrine soliton. In this Letter, we present genuine 2D RWs of the DS II equation, decaying as $O(1/r'^2)$, for a given time t , where prime denotes the moving reference frame (see below). Unlike higher-order multi-pole lumps [45] whose maximum amplitude approaches to a nonzero constant as $t \rightarrow \pm\infty$, here we present two kinds of solutions featuring different asymptotic behaviors for large $|t|$: (i) the maximum value of the first-order RW decays $\sim 1/r'$ to 0, which guarantees that this is indeed a RW wave “appearing from nowhere and disappearing without a trace” [15]; (ii) a RW-lump solution, whose maxima consist of a central peak given by a lump, and an outer ring given by a RW, which eventually reduces to a lump of constant amplitude for large t .

Analysis. In what follows we provide an outline of the methods and give the main results. We start by recalling the Lax pair and Darboux transformation (DT) for the DS II equation [50–52]. The relevant Lax pair is [50, 52]:

$$\Psi_y = J\Psi_x + U\Psi, \quad \Psi_t = 2J\Psi_{xx} + 2U\Psi_x + V\Psi, \quad (2)$$

with a constant diagonal matrix $J = \begin{pmatrix} i & 0 \\ 0 & -i \end{pmatrix}$, and two potential matrices:

$$U = \begin{pmatrix} 0 & u \\ v & 0 \end{pmatrix}, V = \begin{pmatrix} (w + iQ)/2 & u_x - iu_y \\ v_x + iv_y & (w - iQ)/2 \end{pmatrix}. \quad (3)$$

Here, the eigenfunction $\Psi = (\psi, \phi)^T$ (T denotes transpose), the potentials $u, v = ku^* \in \mathbb{C}$, and the field $Q = 2\kappa|u|^2 + S \in \mathbb{R}$, are functions of the three variables x, y, t . As is typically the case in such integrable models, the DS II equation is obtained from the compatibility of the Lax pair, i.e., $\Psi_{yt} = \Psi_{ty}$. Since S and Q are two auxiliary functions in the DS II and its Lax pair, below we will focus on the u waveform.

The construction of the N -fold DT of the DS II equation, necessitates N eigenfunctions $\Psi_k = (\psi_k, \phi_k)^T$ ($k = 1, 2, \dots, N$) and $\tilde{\Psi}_k = (\phi_k^*, \kappa\psi_k^*)^T$, which are associated with a given “seed” solution u and v , of the Lax pair equation (2). The N -th order solution [52] of the DS II equation generated by the N -fold DT reads:

$$u^{[N]} = u + 2i \frac{\delta_2}{\delta_1}, \quad (4)$$

where δ_1 and δ_2 are two determinants of $\Psi_k = (\psi_k, \phi_k)^T$ and $\tilde{\Psi}_k = (\phi_k^*, \kappa\psi_k^*)^T$ (see the Supplemental Material S_1). The line RWs were constructed in Ref. [52]. As mentioned above, the defocusing DS II model, for $\kappa = 1$, has no smooth rational solutions; thus, hereafter, we focus on the focusing case, and fix $\kappa = -1$.

We are now in a position to construct RW solutions u of the DS II equation starting from a zero seed solution, $u = 0, v = 0, Q = 0, w = 0$, of Eq. (4) by the DT method. It is crucial to find proper eigenfunctions Ψ_k associated with the zero seed solution in the Lax pair equation (2) in order to find RWs. Substituting this seed back into Eq. (2), we get a basic eigenfunction Ψ , namely:

$$\begin{aligned} \psi &= \psi(b_1, x, y, t) = a_1 \exp[ib_1(x + iy - 2b_1t)], \\ \phi &= \phi(b_2, x, y, t) = a_2 \exp[ib_2(x - iy + 2b_2t)], \end{aligned} \quad (5)$$

where

$$\begin{aligned} a_1 &= \exp[b_1(s_0 + s_1\epsilon + s_2\epsilon^2 + \dots + s_N\epsilon^N)], \\ a_2 &= \exp[b_2(s_0 + s_1\epsilon + s_2\epsilon^2 + \dots + s_N\epsilon^N)], \end{aligned} \quad (6)$$

are two overall factors added intentionally in order to introduce more expansion coefficients s_i . Importantly, the two components ψ and ϕ in the basic eigenfunction Ψ are independent from each other under the condition of zero seed solution. Performing a Taylor expansion for the above basic eigenfunction Ψ at $(\lambda_1, \lambda_2)^T$ we obtain:

$$\begin{aligned} \psi(\lambda_1 + \epsilon) &= \psi^{[0]} + \psi^{[1]}\epsilon + \dots + \psi^{[N]}\epsilon^N + O(\epsilon^{N+1}), \\ \phi(\lambda_2 + \epsilon) &= \phi^{[0]} + \phi^{[1]}\epsilon + \dots + \phi^{[N]}\epsilon^N + O(\epsilon^{N+1}), \end{aligned} \quad (7)$$

where $\psi^{[k]} = \frac{1}{k!} \frac{\partial^k \psi}{\partial b_1^k} \big|_{b_1=\lambda_1}$, $\phi^{[j]} = \frac{1}{j!} \frac{\partial^j \phi}{\partial b_2^j} \big|_{b_2=\lambda_2}$ ($k, j = 0, 1, 2, \dots, N$). By a tedious calculation, we find that $(\psi^{[k]}, \phi^{[j]})^T$ are analytical and infinitely many eigenfunctions of Lax pair equation (2) are associated with the zero seed solution; this is a novel analytical structure of eigenfunctions of the Lax pair for the DS II equation. Due to the independence of ψ and ϕ , these eigenfunctions are classified in two categories, i.e., $(\psi^{[k]}, \phi^{[k]})^T$ and $(\psi^{[k]}, \phi^{[j]})^T$ ($k \neq j$). Note that $\psi^{[k]}$ contains $k+1$ parameters s_p ($p = 0, 1, 2, \dots, k$) and λ_1 , while $\phi^{[j]}$ contains $j+1$ parameters s_p ($p = 0, 1, 2, \dots, j$) and λ_2 . Below, for simplicity, we set $s_0 > 0$, $s_j = 0$ ($j \geq 1$), and $\lambda_1 = \lambda_2 = i\lambda$ ($\lambda \in \mathbb{R}$). Furthermore, hereafter, all results are discussed in a moving reference frame, i.e., $x' = x$, $y' = y + 4\lambda t$ and $r' = \sqrt{x'^2 + y'^2}$, which is more convenient in order to investigate the properties of the obtained solutions.

To derive rational solutions $u^{[N]}$ of the DS II equation, we select $\Psi_k = (\psi_k, \phi_k)^T = (\psi^{[2k-1]}, \phi^{[2k-1]})^T$ ($k = 1, 2, \dots, N$) in Eq. (4). Setting $N = 1$ and $\lambda = 1$, Eq. (4) yields a usual first-order lump, $u_{\text{lump}}^{[1]} = -\frac{2s_0 e^{2i(2t-y')}}{x'^2 + y'^2 + s_0^2}$, and its maximum value $|u_{\text{lump}}^{[1]}| = \frac{2}{s_0}$. Setting $N = 2$ and $\lambda = 1$, Eq. (4) yields a second-order rational solution $u^{[2]}$, corresponding to the first-order RW of the DS II, namely:

$$u_{\text{rw}}^{[1]} = \frac{6s_0 N_{\text{rw}}}{D_{\text{rw}}} e^{-2i(2t+y')}, \quad (8)$$

where

$$\begin{aligned} N_{\text{rw}} &= -x'^4 + y'^4 - 2s_0^2 x'^2 + 4s_0^2 y'^2 - s_0^4 + \\ &\quad 12it(x'^2 + y'^2 + s_0^2), \\ D_{\text{rw}} &= (x'^2 + y'^2 + s_0^2)^3 + 12s_0^2(x'^2 + s_0^2)y'^2 + 144s_0^2 t^2. \end{aligned}$$

The solution $u_{\text{rw}}^{[1]}$ is a smooth and nonsingular RW as $s_0 > 0$ on zero background, with the following properties:

- The modulus $|u_{\text{rw}}^{[1]}|$, which is an even function, decays algebraically like $O(\frac{1}{r'^2})$ for any given time t .
- When $r' = \sqrt{x'^2 + y'^2} = 0$, the RW solution $u_{\text{rw}}^{[1]}$ reduces to:

$$u_{\text{rwc}}^{[1]} = \frac{(-6s_0^3 + 72is_0 t)e^{-4it}}{s_0^4 + 144t^2}. \quad (9)$$

Notice that $|u_{\text{rwc}}^{[1]}|$ reaches the maximum value $\frac{6}{s_0}$ at $t = 0$ (see Figs. 1(a,d)), while it obtains a (local) minimum value thereafter, and finally decays like $O(\frac{s_0}{2t}) \sim 0$ as $|t| \rightarrow \infty$.

• When $r' \gg 0$, the maxima of $|u_{\text{rw}}^{[1]}|$ form a rectangular curve of different height at an intermediate stage (Figs. 1(b,e)), which eventually morphs into a circle (i.e., a nearly radial pattern) at the final stage of the evolution (Figs. 1(c,f)). At its maximum, the radius of this circle is given by:

$$r' = \sqrt{x'^2 + y'^2} \sim (6s_0\sqrt{2}|t|)^{1/3} \quad (10)$$

as $|t| \rightarrow \infty$, while the corresponding intensity

$$|u_{\text{rwcircle}}^{[1]}|^2 \sim \frac{4}{(3s_0|t|)^{2/3}} \sim \frac{8}{(r')^2} \sim 0, \quad (11)$$

as $|t| \rightarrow \infty$, $r' \rightarrow \infty$.

The symmetry and extreme values of the intensity with $s_0 = 1$ can be verified by the snapshots shown in Fig. 1, for $t = 0, 1, 200$. Note that only profiles for $t \geq 0$ are shown because $|u_{\text{rw}}^{[1]}|$ is an even function of t . The red solid circles denote the maxima of $|u_{\text{rw}}^{[1]}|$, which are plotted by using the exact formulation $\frac{6}{s_0}$ for $t = 0$, and the approximate formulas r' and $|u_{\text{rwcircle}}^{[1]}|$ for $t \neq 0$. There exists a deviation between the red solid circles and the maxima in Fig. 1(e) because time t is too small for the asymptotics to be valid. This deviation disappears in Fig. 1(f) for (sufficiently) large time $t = 200$, which is well within the asymptotic regime of Eq. (10).

An animation [53] is provided in the Supplementary Material showing the dynamical evolution of the first order RW, which can be summarized as follows. At the early stage of the evolution, for large and negative t , $|u_{\text{rw}}^{[1]}|$ appears from the background as a wide circle of low intensity; gradually, it converges to a rectangular column with four maxima on its top at the intermediate stage, and then a large peak at $t = 0$. Next, the RW follows the reverse path, initially dispersing and eventually reverting back to a nearly radial form for large and positive t .

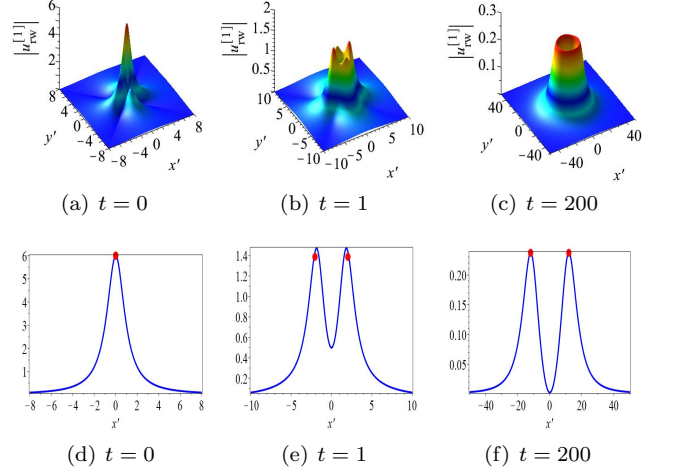


FIG. 1. (Color online) Top panels: Profiles of the first-order RW $|u_{\text{rw}}^{[1]}|$ in the (x', y') - plane with parameters $s_0 = 1$ at $t = 0, 1, 200$, respectively. Bottom panels: The corresponding cross-sectional profiles of the top panels along x' -axis. The red solid circles are plotted using the exact formulation $\frac{6}{s_0}$ for $t = 0$, and the approximate formulas r' and $|u_{\text{rwcircle}}^{[1]}|$ for $t \neq 0$.

Here it should be pointed out that the first order RW $u_{\text{rw}}^{[1]}$ is very different from the multi-pole lump [45] of the DS II, because the latter has a non-vanishing amplitude as $|t| \rightarrow \infty$. In addition, this RW solution is naturally also different from the line RW [42] of the DS II, since the latter is not doubly localized in both x and y , but only in one of the two (in the other, it features a line profile).

Extending this approach to $N = 3$, Eq. (4) yields a third-order rational solution, which is an unprecedented (to the best of our knowledge) RW-lump solution $u_{\text{rw-lump}}$ of the DS II equation. The explicit expression of $u_{\text{rw-lump}}$ [53] is given in the Supplementary Material S₂. Here, we describe its principal dynamical properties.

- The modulus $|u_{\text{rw-lump}}|$, which is an even function, decays algebraically like $O(\frac{1}{r'^2})$ for any given time t .
- When $r' = 0$, the solution $u_{\text{rw-lump}}$ reduces to

$$u_{\text{rw-lumpc}} = \frac{12(-s_0^4 + 60t^2 + 10is_0^2 t)e^{-4i\lambda^2 t}}{s_0(s_0^4 + 360t^2 + 60is_0^2 t)}. \quad (12)$$

The modulus $|u_{\text{rw-lumpc}}|$ reaches the maximum value $\frac{12}{s_0}$ at $t = 0$ (Figs. 2(a,d)), as a result of the interaction of the RW and the lump. Then, it returns to maximum value of the first-order lump, i.e., $|u_{\text{lumpM}}^{[1]}| \sim \frac{2}{s_0}$, as the RW disappears for $|t| \rightarrow \infty$.

• For $r' \gg 0$, maxima of $|u_{\text{rw-lump}}|$ form a rectangular curve at the intermediate stage (Figs. 2(b,e)), which subsequently reverts to a radial outgoing structure at the final stage (Figs. 2(c,f)) of the evolution –in addition to the persisting lump at the center. At its maximum, the radius of this circle is given by:

$$r' = \sqrt{x'^2 + y'^2} \sim (288s_0|t|^2)^{1/5}, \quad (13)$$

as $|t| \rightarrow \infty$, while the intensity at this circle is:

$$|u_{\text{rw-lump-circle}}|^2 \sim \frac{2\sqrt{3}^{\frac{2}{5}}}{(s_0|t|^2)^{\frac{2}{5}}} \sim \frac{24}{(r')^2}, \quad (14)$$

as $|t| \rightarrow \infty$, $r' \rightarrow \infty$.

It is worth observing that the maxima of $|u_{\text{rw-lump}}|$ can be decomposed into $|u_{\text{lumpM}}^{[1]}| + |u_{\text{rw-lump-circle}}| \sim \frac{2}{s_0} + \frac{2\sqrt{6}}{r'}$ for $|t| \gg 0$, supporting the asymptotic decomposition into a lump and a RW as discussed above. Fig. 2 presents the relevant features through the snapshots of different times ($t = 0, 2, 200$), incorporating where possible predictions of the analytical formula, such as the location of the RW circle for large t . The animation provided in [53] shows the dynamical evolution of the RW-lump. One can discern that: (a) a lump in the center always exists; (b) a RW appears as an outer ring from the background at an early stage, then converges gradually to the origin of coordinate as a large peak, (c) later, the RW is dispersed to a circle, and finally disappears into the background again as $|t| \rightarrow \infty$.

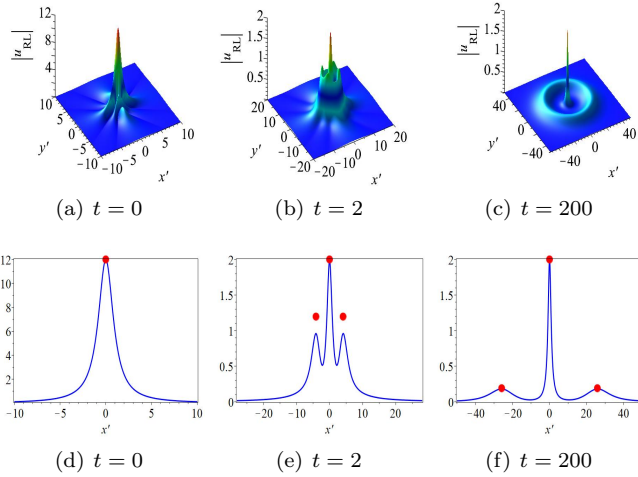


FIG. 2. (Color online) Top panels: Profiles of the rogue wave-lump $|u_{\text{rw-lump}}|$ ($|u_{\text{RL}}|$ in this figure for convenience) in the (x', y') -plane with parameters $s_0 = \lambda = 1$ at $t = 0, 2, 200$, respectively. Bottom panels: The corresponding cross-sectional profiles of the top panels along x' -axis. The red solid circles are plotted using the exact formulation $\frac{12}{s_0}$ for $t = 0$, and the approximate formulas $\frac{2}{s_0}(r' = 0)$ and $\frac{2\sqrt{6}}{r'}(r' \neq 0)$ for $t \neq 0$.

Higher-order RWs and RW-lumps of the DS II equation can be constructed by even-fold and odd-fold DT, respectively. For instance, a second-order RW $|u_{\text{rw}}^{[2]}|$, which is constructed by setting $N = 4$ in Eq. (4), is plotted in Fig. 3 (see also an animation [53]) with $s_0 = \lambda = 1$. Both Fig. 3 and the animation demonstrate again the appearance, convergence (to $r' = 0$), and then dispersion, and disappearance of the RW. Compared with $u_{\text{rw}}^{[1]}$, the second-order RW has (i) higher amplitude, and (ii) two rings of intensity maxima for large time t . Between

them, these harbor a 2D RW hole (see Fig.3(e,f)) during the evolution process. It is interesting to notice that a 1D RW hole of the NLS equation has been experimentally observed in a water tank [54].

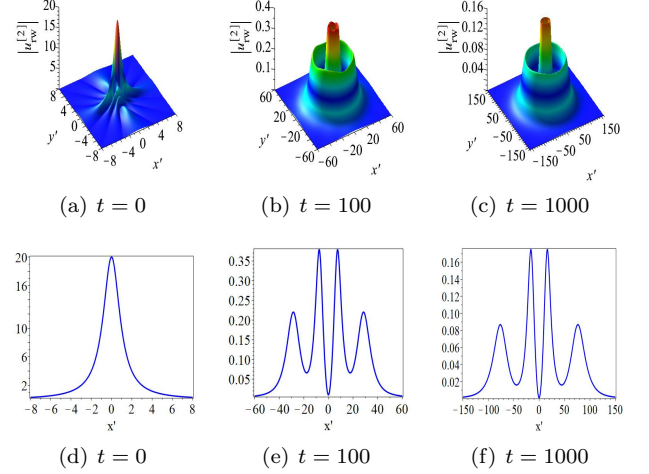


FIG. 3. (Color online) Top panels: Profiles of the second-order RW $|u_{\text{rw}}^{[2]}|$ in the (x', y') -plane, for $s_0 = \lambda = 1$ at $t = 0, 100, 1000$, respectively. Bottom panels: The corresponding cross-sectional profiles of top panels along x' -axis.

Conclusions. We have reported an unprecedented analytical structure of eigenfunctions of the Lax pair associated with the zero seed solution for the DS II equation. Substituting these new eigenfunctions into the even-fold DT, we found genuine 2D RWs of the DS II equation. We have thus addressed the long-standing problem of the construction of RWs on zero background for DS II, and provided a proper candidate to describe fluid RWs by means of a canonical 2D generalization of the Peregrine soliton of the 1D NLS equation. The RWs were localized both in space and time, that is, as $|t|$ and $r' \rightarrow \infty$, their maximum amplitude decayed to 0 as $1/r'$. As a byproduct, RW-lump solutions of the DS II have been shown to be generated by odd-fold DT, which is localized in space only, because one-lump of this solution located at the origin approaches $\frac{2}{s_0}$ as $|t| \rightarrow \infty$. Multi-ring RWs (obtained through higher-order expansions) also exist and feature RW holes between them.

We expect that these findings may motivate research efforts towards the generation of 2D RWs in large water tanks and optical systems, in a multi-dimensional extension of recent 1D experimental efforts, and paving new directions for RW research. Moreover, much like line solitons of the KP II equation, which have been used to explain shallow water wave patterns [55], the RWs of the DS II can also be used for similar studies on ocean waves—since both KP II and DS II are pertinent to shallow water with weak surface tension, and DS II can be derived from KP II [9].

Acknowledgments. This work was supported by the National Natural Science Foundation of China (Grants

11671219 and 11871446) and the Natural Science Foundation of Zhejiang Province (Grants LZ19A010001 and LSY19A010002). P.G.K. and D.J.F. acknowledge that

this work was made possible by NPRP Grant No.8-764-1-160 from Qatar National Research Fund (a member of Qatar Foundation).

-
- [1] E. Pelinovsky and C. Kharif, *Extreme Ocean Waves* (Springer, Berlin, 2008).
 - [2] K. Dysthe, H. E. Krogstad, and P. Müller, *Annu. Rev. Fluid Mech.* **40**, 287 (2008).
 - [3] A. Osborne, *Nonlinear Ocean Waves and the Inverse Scattering Transform* (Elsevier, New York, 2010).
 - [4] S. Chen, F. Baronio, J.M. Soto-Crespo, P. Grelu, D. Mihalache, *J. Phys. A: Math. Theor.* **50**, 463001 (2017).
 - [5] A. Davey and K. Stewartson, *Proc. R. Soc. Lond. A* **338**, 101 (1974).
 - [6] V. D. Djordjević and L. G. Redekopp, *J. Fluid Mech.* **79**, 703 (1977).
 - [7] M. J. Ablowitz and H. Segur, *J. Fluid Mech.* **92**, 691 (1979).
 - [8] M. J. Ablowitz and H. Segur, *Solitons and the Inverse Scattering Transform* (SIAM, Philadelphia, PA, 1981), Chapter 4.3b.
 - [9] M. J. Ablowitz, *Nonlinear Dispersive Waves: Asymptotic Analysis and Solitons* (Cambridge University Press, Cambridge, 2011), Chapter 6.8.
 - [10] W. Craig, U. Schanz, and C. Sulem, *Ann. Inst. Henri Poincaré Anal. Nonlinéaire* **14**, 615 (1997).
 - [11] C. Sulem and P.L. Sulem, *The Nonlinear Schrödinger Equation* (Springer-Verlag New York, 1999).
 - [12] M.J. Ablowitz, B. Prinari and A.D. Trubatch, *Discrete and Continuous Nonlinear Schrödinger Systems* (Cambridge University Press, Cambridge, 2004).
 - [13] D. H. Peregrine, *J. Aust. Math. Soc. Ser. B* **25**, 16 (1983).
 - [14] N. N. Akhmediev, V. M. Eleonskii, and N. E. Kulagin, *Sov. Phys. JETP* **62**, 894 (1985).
 - [15] N. Akhmediev, A. Ankiewicz, and M. Taki, *Phys. Lett. A* **373**, 675 (2009).
 - [16] D. J. Kedziora, A. Ankiewicz, and N. Akhmediev, *Phys. Rev. E* **84**, 056611 (2011).
 - [17] D. J. Kedziora, A. Ankiewicz, and N. Akhmediev, *Phys. Rev. E* **88**, 013207 (2013).
 - [18] J. S. He, H. R. Zhang, L. H. Wang, K. Porsezian, and A. S. Fokas, *Phys. Rev. E* **87**, 052914 (2013).
 - [19] L. H. Wang, J. S. He, H. Xu, J. Wang, and K. Porsezian, *Phys. Rev. E* **95**, 042217 (2017).
 - [20] B. Kibler, J. Fatome, C. Finot, G. Millot, F. Dias, G. Genty, N. Akhmediev, and J. M. Dudley, *Nat. Phys.* **6**, 790 (2010).
 - [21] K. Hammani, B. Kibler, C. Finot, P. Morin, J. Fatome, J. M. Dudley, and G. Millot, *Opt. Lett.* **36**, 112 (2011).
 - [22] J. M. Dudley, F. Dias, M. Erkintalo, and G. Genty, *Nat. Photonics* **8**, 755 (2014).
 - [23] B. Frisquet, B. Kibler, P. Morin, F. Baronio, M. Conforti, and B. Wetzol, *Sci. Rep.* **6**, 20785 (2016).
 - [24] A. Chabchoub, N. P. Hoffmann, and N. Akhmediev, *Phys. Rev. Lett.* **106**, 204502 (2011).
 - [25] A. Chabchoub, N. Hoffmann, M. Onorato, A. Slunyaev, A. Sergeeva, E. Pelinovsky, and N. Akhmediev, *Phys. Rev. E* **86**, 056601 (2012).
 - [26] A. Chabchoub, *Phys. Rev. Lett.* **117**, 144103 (2016).
 - [27] A. R. Osborne, M. Onorato, and M. Serio, *Phys. Lett. A* **275**, 386 (2000).
 - [28] A. Kundu, A. Mukherjee, T. Naskar, *Proc. R. Soc. A* **470**, 20130576 (2014).
 - [29] A. S. Fokas and M. J. Ablowitz, *J. Math. Phys.* **25**, 2494 (1984).
 - [30] A. S. Fokas and V. E. Zakharov (Eds.), *Important Developments in Soliton Theory* (Springer, Berlin, 1993).
 - [31] M. J. Ablowitz and P. A. Clarkson, *Solitons, Nonlinear Evolution Equations and Inverse Scattering* (Cambridge University Press, Cambridge, 1991).
 - [32] S. L. Musher, A. M. Rubenchik, and V. E. Zakharov, *Phys. Rep.* **129**, 285 (1985).
 - [33] K. Nishinari, K. Abe, and J. Satsuma, *J. Phys. Soc. Jpn.* **62**, 2021 (1993).
 - [34] C. S. Panguetna, C. B. Tabi, and T. C. Kofané, *Phys. Plasmas* **24**, 092114 (2017).
 - [35] A. C. Newell and J. V. Moloney, *Nonlinear Optics* (Addison-Wesley, Redwood City, CA, 1992).
 - [36] H. Leblond, *J. Phys. A: Math. Gen.* **31**, 5129 (1998).
 - [37] H. Leblond, *Phys. Rev. Lett.* **95**, 033902 (2005).
 - [38] H. Leblond, *J. Phys. A: Math. Gen.* **32**, 7907 (1999).
 - [39] R. Beals and R. R. Coifman, *Physica D* **18**, 242 (1986).
 - [40] J. Satsuma and M. J. Ablowitz, *J. Math. Phys.* **20**, 1496 (1979).
 - [41] V. A. Arkadiev, A. K. Pogrebkov, *Physica D* **36**, 189 (1989).
 - [42] Y. Ohta and J. Yang, *J. Phys. A: Math. Theor.* **46**, 105202 (2013).
 - [43] A. S. Fokas, D. E. Pelinovsky, and C. Sulem, *Physica D* **152**, 189 (2001).
 - [44] M. Mañas and P. Santini, *Phys. Lett. A* **227**, 325 (1997).
 - [45] J. Villarroel and M. J. Ablowitz, *SIAM J. Math. Anal.* **34**, 1253 (2003).
 - [46] J. Villarroel and M. J. Ablowitz, *Phys. Rev. Lett.* **78**, 570 (1997).
 - [47] J. Villarroel, J. Prada, and P. G. Estévez, *J. Phys. A: Math. Theor.* **50**, 495203 (2017).
 - [48] T. Arai, K. Takeuchi, and M. Tajiri, *J. Phys. Soc. Jpn.* **70**, 55 (2001).
 - [49] T. Arai and M. Tajiri, *J. Phys. Soc. Jpn.* **84**, 024001 (2015).
 - [50] V. B. Matveev and M. A. Salle, *Darboux Transformations and Solitons* (Springer, Berlin, 1991).
 - [51] C. H. Gu, H. S. Hu, and Z. X. Zhou, *Darboux Transformations in Integrable Systems: Theory and Their Applications to Geometry* (Springer, Berlin, 2005).
 - [52] K. Xin, *Rogue Wave Solutions to Integrable System by Darboux Transformation* (Master's thesis, Department of Mathematics and Statistics, University of Vermont, USA, October, 2014).
 - [53] See Supplemental Material at <http://xxx>. for dynamical evolution and formulas of rational solutions of the DS II. More specifically, we give there: (1) The expressions of two determinants δ_1 and δ_2 (see the Supplemental Material S_1). (2) The movie 13-3Danimationrw.gif that shows the dynamical evolution of the first-order RW given by

equation (8) with parameter $s_0 = 1$ from $t = -200$ to $t = 200$. (3) The analytical expression of the rogue wave-lump solution $u_{\text{rw-lump}}$ of the DS II, which is generated by the three-fold DT (see the Supplemental Material S_2). (4) The movie 135-3Danimationrwlump.gif which displays the dynamical evolution of the rogue wave-lump solution $u_{\text{rw-lump}}$ given in S_2 with parameters $\lambda = 1$ and $s_0 = 1$ from $t = -200$ to $t = 200$. (5) The movie 1357-

3Danimation2rw.gif shows the dynamical evolution of the second order RW of the DS II with parameters $\lambda = 1$ and $s_0 = 1$ from $t = -1000$ to $t = 1000$.

- [54] A. Chabchoub, N. P. Hoffmann, and N. Akhmediev, J. Geophys. Res. **117**, C00J02 (2012).
- [55] M. J. Ablowitz and D. E. Baldwin, Phys. Rev. E **86**, 036305 (2012).